

X-RAY AND RADIO PROPERTIES OF SOLAR ^3He -RICH EVENTS

D. V. REAMES, B. R. DENNIS, AND R. G. STONE
 NASA/Goddard Space Flight Center

AND

R. P. LIN
 Space Sciences Laboratory, University of California, Berkeley
 Received 1987 June 29; accepted 1987 September 30

ABSTRACT

We have examined radio and X-ray properties of solar flares associated with a new sample of individual ^3He -rich solar particle events. Given the association between kilometric type III bursts and ^3He -rich events, the timing of the radio events is used to identify the related X-ray increases. The X-ray events exhibit a rich variety, from the standpoint of both intensity and complexity. Examination of the events shows statistically significant anticorrelations between the $^3\text{He}/^4\text{He}$ ratio and the intensity of the event as measured at kilometric wavelengths and in hard and soft X-rays; larger $^3\text{He}/^4\text{He}$ ratios occur in smaller flares. The result suggests that a coupling may exist between the pre-heating phase and the acceleration phase of these events or that mixing occurs between an enriched particle population accelerated within the compact flare and a normal population accelerated by a shock propagating away from an intense flare.

Subject headings: Sun: flares — Sun: radio radiation — Sun: X-rays

I. INTRODUCTION

For many years the properties of the small and elusive ^3He -rich solar particle events could be observed only by integrating particle intensities for periods of many hours (see e.g., Ramaty *et al.* 1980; Kocharov and Kocharov 1984). Therefore, these early “events” frequently combined the output of several solar flares with differing intensities and composition.

Using more sensitive instrumentation on *ISEE 3*, Reames, von Rosenvinge and Lin (1985, hereafter RvL) were able to resolve ^3He -rich periods into sequences of individual events, each accompanied by an electron increase. The precise timing of the electron increases could be used to determine the time of the parent flare with an accuracy of a few minutes. The kilometric type III radio emission produced by these same electrons was used by Reames and Stone (1986) to extend the list of well-identified ^3He -rich solar flares and to study the relationship of flares within a group.

Some of the source properties of the first portion of this new list of ^3He -rich flares were examined by Kahler *et al.* (1987). The events were found to be associated with small, compact H α flares.

In the present paper we examine, for the first time, the source properties of the complete new list of individual ^3He -rich solar flares. The same type III radio emission used to identify the events provides the timing required to select the associated hard and soft X-ray increases.

II. OBSERVATIONS

Particle and radio observations were made aboard the *ISEE 3* spacecraft and have been described extensively in RvL and in Reames and Stone (1986).

Both soft and hard X-rays were also measured aboard *ISEE 3* by the Berkeley X-ray Spectrometer (Anderson *et al.* 1978) that covers the energy region above about 5 keV. These data were supplemented with lower-energy soft X-ray observations from the *GOES* spacecraft and with hard X-ray measurements made with the Hard X-Ray Burst Spectrometer (HXRBS;

Orwig, Frost and Dennis 1980) on the *Solar Maximum Mission (SMM)*. A recent summary of measurements from the HXRBS instrument is given by Dennis (1985).

Parameters of the 31 ^3He -rich events are given in Table 1. Kilometric radio observations were available for 27 events, and all of these had strong kilometric type III bursts.

Soft X-ray observations were made at 30 of the ^3He -rich event times with either *ISEE*, *GOES*, or both. In this sample, 22 events showed soft X-ray increases, five occurred during times of high background, and three showed no increase above the quiescent instrument background.

Of the 12 events that were observable with *SMM*, 11 had hard X-ray emission and are listed in the HXRBS catalog (Dennis *et al.* 1985; one of the 11 events is partially eclipsed). The *ISEE* instrument detected hard X-rays in 14 of 24 possible events. Much of this apparent discrepancy occurs because events in the sample reported by RvL were smaller than those in the later sample reported by Reames and Stone (1986) and because *SMM* observations exist only during this latter period. Overall, hard X-ray increases were seen in 15 of 26 possible events.

For each of the events, plots like those shown in Figures 1–4 were prepared to study the event timing. The example in Figure 1 shows the time histories of the hard X-rays in the center panel with the radio and soft X-ray data in the upper and lower panels, respectively. Extrapolation of the radio data back to the time of the hard X-ray peak is clear in this figure. (Note that 2 MHz corresponds to about 6 R_{\odot}). In more complex events, the timing of the dominant radio peak was used to select the correct X-ray increase or to provide the event onset time in cases where hard X-ray data were absent.

Figures 2 and 3 show the profiles of two larger, more complex events. The two events differ in the relative size and duration of the hard and soft X-ray components. In sharp contrast is the 1979 May 17 event shown in Figure 4. This event produced the large ^3He increase studied extensively by RvL, but, as seen in Figure 4, there is little or no soft X-ray

TABLE 1
X-RAY AND RADIO PROPERTIES OF ³He-RICH FLARES

Date	Flare Onset UT	³ He/ ⁴ He Ratio	³ He Flux (1)	GOES Peak (2)	5keV Flux (3)	E.M. Temp (4)	ISEE-3 25keV Peak (6)	Peak (6)	Peak (6)	HXRBS Total counts	III Int (7)	2 MHz Int (7)	H α Site Imp Region
78 Nov 8	1751	0.36±0.10	20	C5.7	9180	184	14.4	400	3	11.9	N18E12 1B 15643
78 Nov 27	2055	26 ^{+∞} -10	20	C1.0	503	22.4	12.6	<10	3	8.6	N26W47 -B 15672
78 Dec 26	1319	3.1±0.6	200	<C1	48	<10	0	9.2	S21W45 -F 15721
78 Dec 26	2122	0.8±0.2	100	<C1	<10	<10	0	8.3	N12W90 -N 15802
79 Feb 10	1817	0.68±0.10	150	<C3	<60	<10	0	9.7	S35W78 -F 15996
79 May 17	0551	12 ^{+∞} -2	300	<C2	240	26.0	9.58	<10	2	9.3	S17W48 -B 16205
79 Aug 14	2049	0.12±0.02	30	C5.2	5460	112	11.3	60	2	11.3	N20W62 -F 16252
79 Sep 6	0907	2.0 ^{+2.3} -1.4	10	C1	201	4.23	12.9	<10	2	10.0	N17W65 -F 16252
79 Sep 6	1139	2.4 ^{+2.8} -1.7	10	...	306	0.95	17.5	<10	3	11.1	N16W63 -N 16252
79 Sep 6	1336	0.26±0.10	40	...	3000	59.3	13.6	40	3	10.9	N16W65 -F 16252
79 Sep 6	1850	0.44±0.10	70	...	<10	<10	2	10.0	N10W51 1B 16490
79 Dec 14	1553	1.5±0.1	2000	C7	13300	223	14.7	40	2	9.4	S14W44 -N 17246
79 Dec 23	1726	2.9±0.2	400	<C1	100	<10	0	10.1	S12W48 -N 17246
80 Nov 9	1622	0.9 ^{+0.8} -0.2	300	C4	5180	135	13.5	~10	90	265	3	9.8	S09W51 -N 17246
80 Nov 9	2028	3.7 ^{+1.8} -0.5	1300	~C3	911	40.4	12.0	~10	63	404	2	10.4	S09W51 -N 17246
80 Nov 10	0446	4 ⁺³ -2	500	~C3	237	3.84	15.7	~10	61	361	2	10.0	S09W51 -N 17246
80 Nov 10	0744	>4	500	<C4	2	8.4	N10W65 1B 17244
80 Nov 11	1605	0.3±0.1	100	<M2	2	...	S12W44 -N 17255
80 Nov 15	1018	>1.6	600	<C3	0	8.3	N07E13 1B 17331
80 Dec 16	1452	0.5±0.1	30	M5	78300	8414	10.7	1600	3958	100000	3	12.5	ambiguous
81 Sep 15	1934	1.2±0.2	250	...	<300	~10	70	646	3	11.5	S06W31 1N 3635
81 Nov 20	1041	0.2±0.1	300	C2.5	2	10.2	S06W34 1B 3635
82 Mar 10	1220	>2.2	600	3	...	N14W50 -B 3781
82 Mar 10	1844	0.7±0.2	300	C5.4	3	...	N17W56 2B 3781
82 Jun 25	0531	0.24±0.04	700	C6.9	4030	94.9	12.2	50	187	6377	3	9.8	...
82 Jun 25	1944	0.36±0.08	1000	M2	51200	8488	10.7	600	1276	59937	3	11.0	...
82 Jun 30	0912	>1.4	150	...	<10	<10	0	8.1	...
82 Aug 13	1814	1.9±0.3	300	C2	186	14530	4.3
82 Aug 13	2259	0.8±0.1	900	C8	40200	47.7	14.3	200	446	31668	3.6	11.3	N11W59 -N 3837
82 Aug 14	0242	1.2±0.1	900	M1.2	37000	483	13.9	350	610	39639	4.9	9.8	N11W60 -B 3837
82 Aug 14	0507	0.24±0.05	...	M4	90600	2650	12.4	120000	>535	>39222	3.7	12.1	N11W62 1B 3837

(1) $10^{-6} / (\text{cm}^2 \text{ster s MeV/AMU})$ (2) CMX units with $C=10^{-6}$ watts/m² and $M=10^{-5}$ watts/m² (3) $1/(\text{cm}^2 \text{s keV})$
 (4) $10^{46} / \text{cm}^3$ (5) 10^6 K (6) counts/s (7) $\log(T_A)$, T_A in K

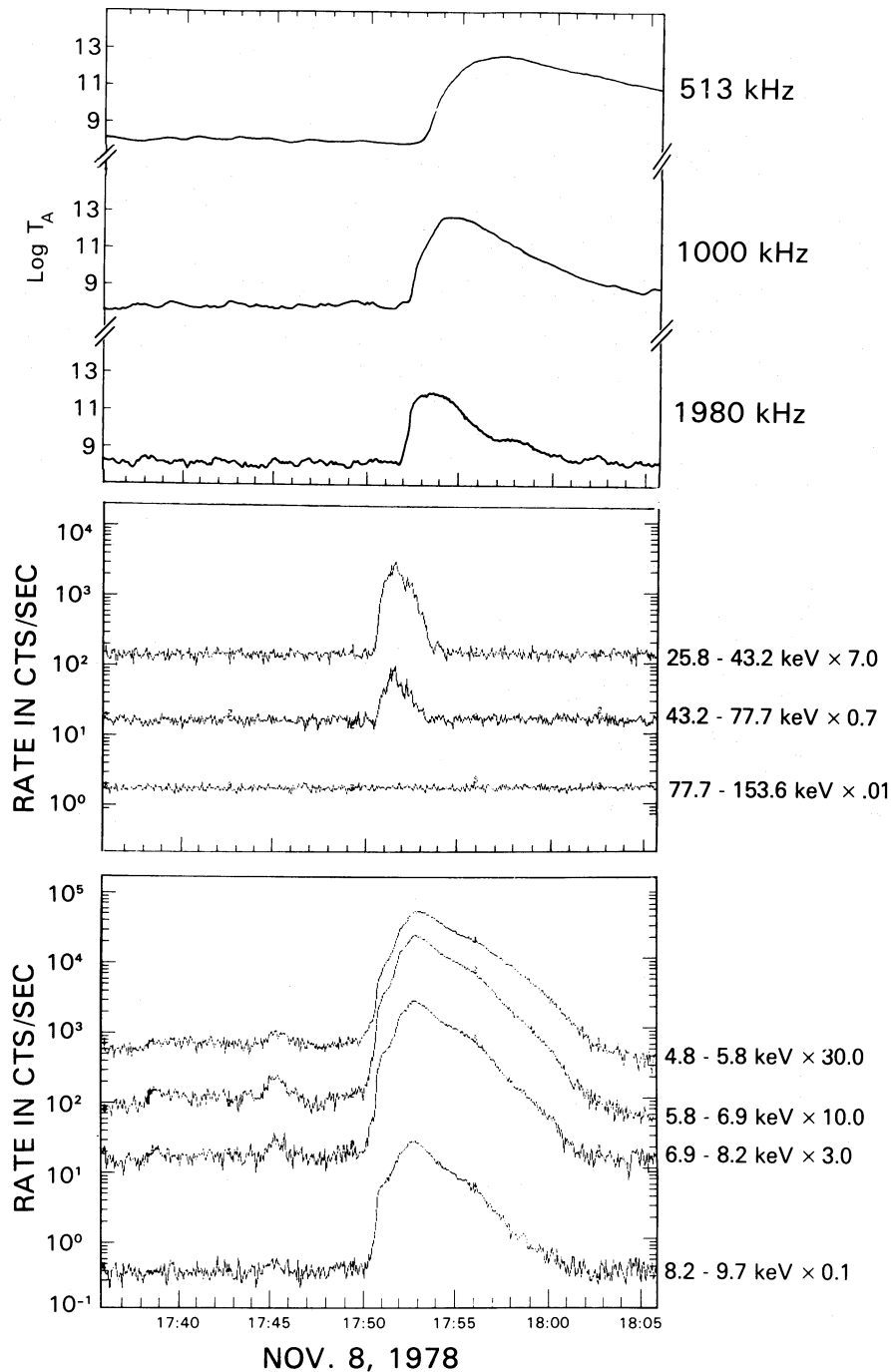


FIG. 1.—*ISEE 3* X-ray and radio timing in the 1978 November 8 ^3He -rich event. The kilometric radio data are shown in the top panel, the hard X-ray measurements, in the center panel, and the soft X-ray data, in the lower panel.

increase and the hard X-ray data have been omitted entirely since they show no increase at all.

In Figure 5 we show the HXRBS data at high time resolution for the event of 1982 August 13 that was shown in Figure 3. The rapid fluctuations seen in Figure 5 are common in these events.

Time scales of the soft-X-ray events, like those shown, were all relatively short, with durations (at 10% of maximum) in the range of 5–10 minutes.

In order to investigate event parameters that might correlate with the observed particle enhancements, we determined the soft X-ray temperature and emission measure from the *ISEE* and *GOES* observations. These parameters were extracted by a least-squares fit of the multichannel *ISEE* data. *GOES* data were analyzed using the expressions given by Thomas, Starr, and Crannell (1985). These expressions include corrections for spectral line emission and nonlinear response of the broadband *GOES* channels.

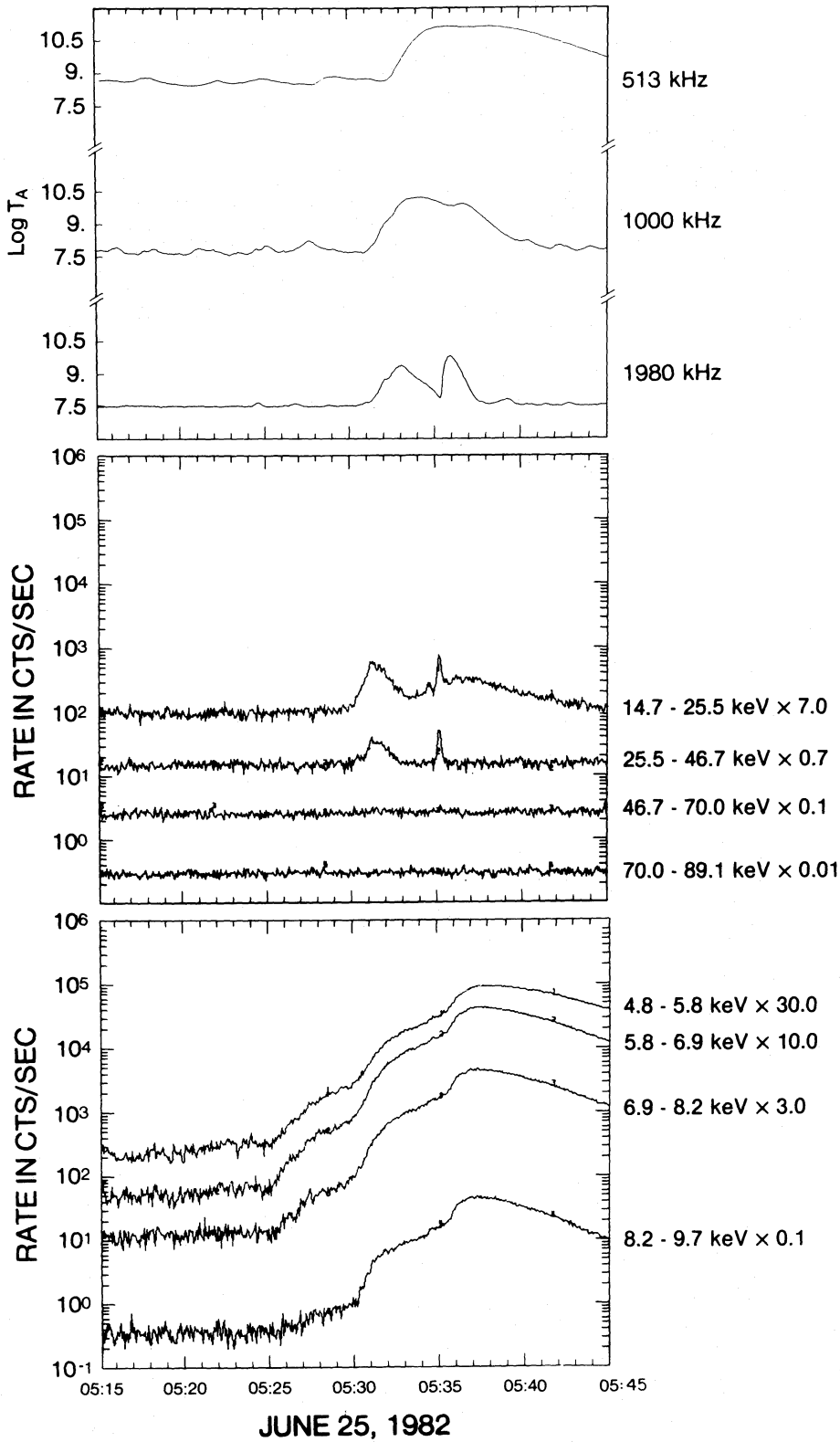


FIG. 2.—*ISEE 3* X-ray and radio timing in the 1982 June 25 ^3He -rich event (see Fig. 1)

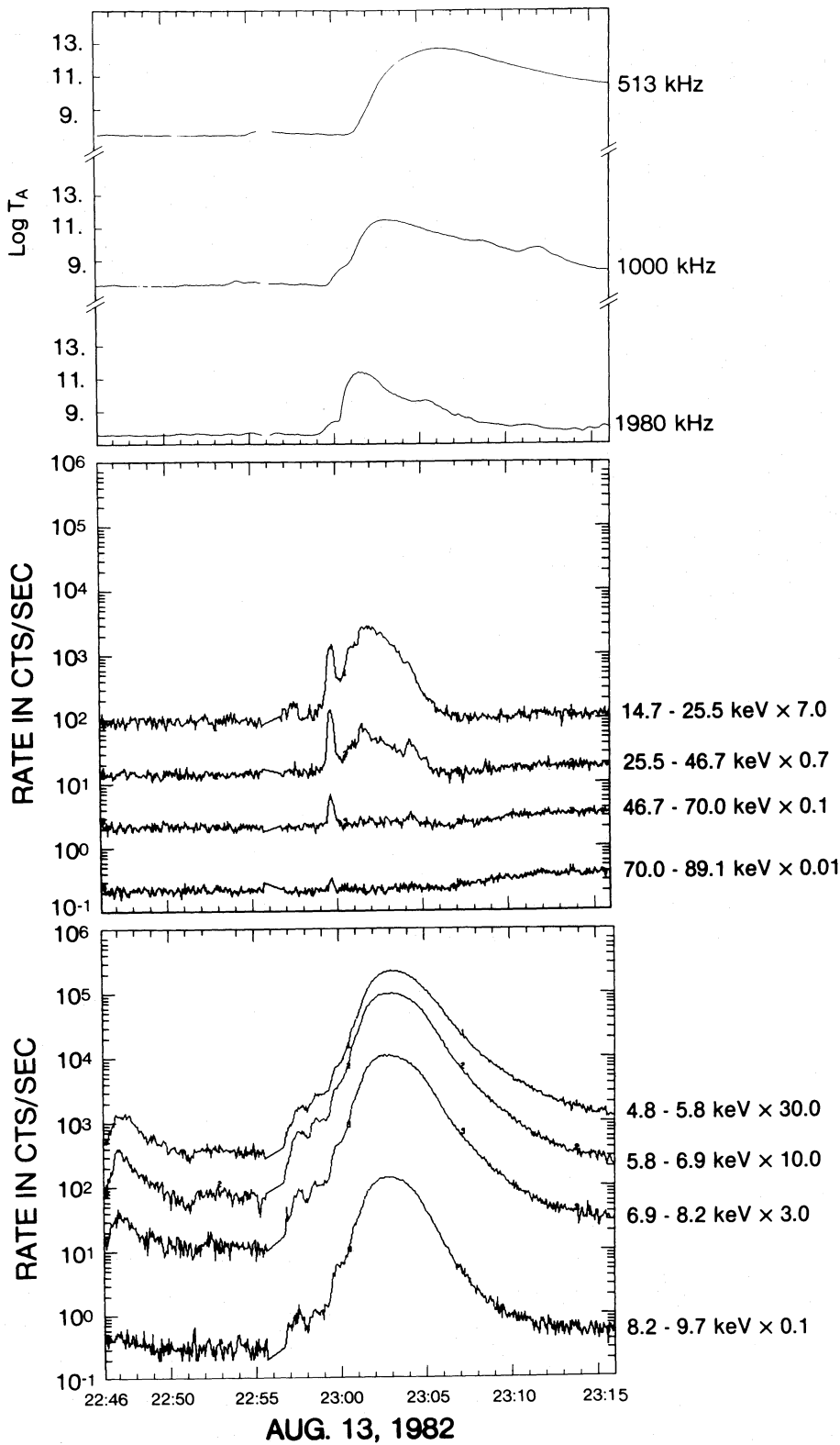


FIG. 3.—*ISEE 3* X-ray and radio timing in the 1982 August 13 ^3He -rich event (see Fig. 1)

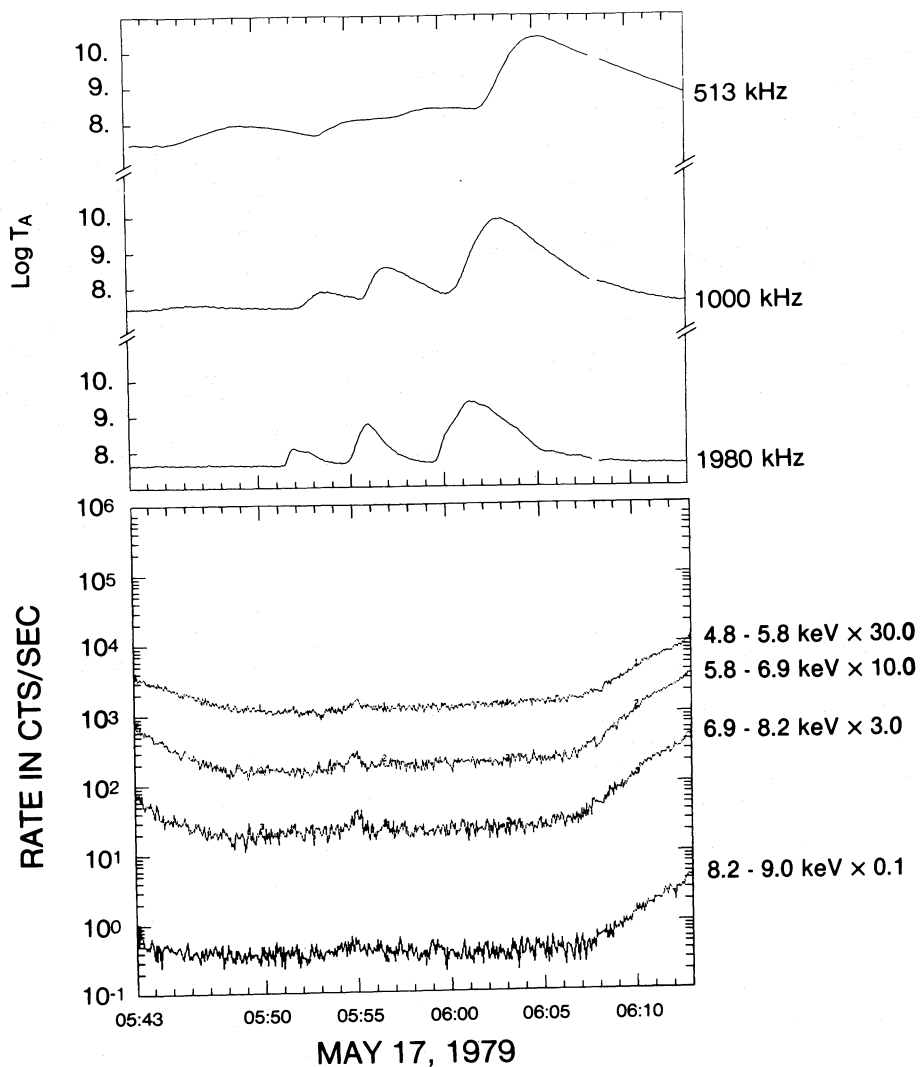


FIG. 4.—*ISEE 3* X-ray and radio timing in the 1979 May 17 ³He-rich event. Kilometric radio data are shown in the top panel, and soft X-ray data, in the lower panel. No hard X-ray event is seen.

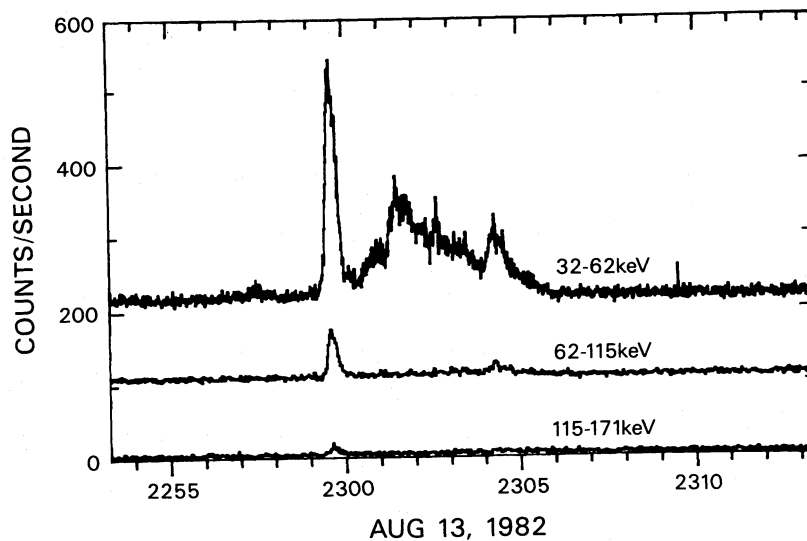


FIG. 5.—HXRBS hard X-ray observations of the 1982 August 13 ³He-rich event observed at higher time resolution than shown in Fig. 3

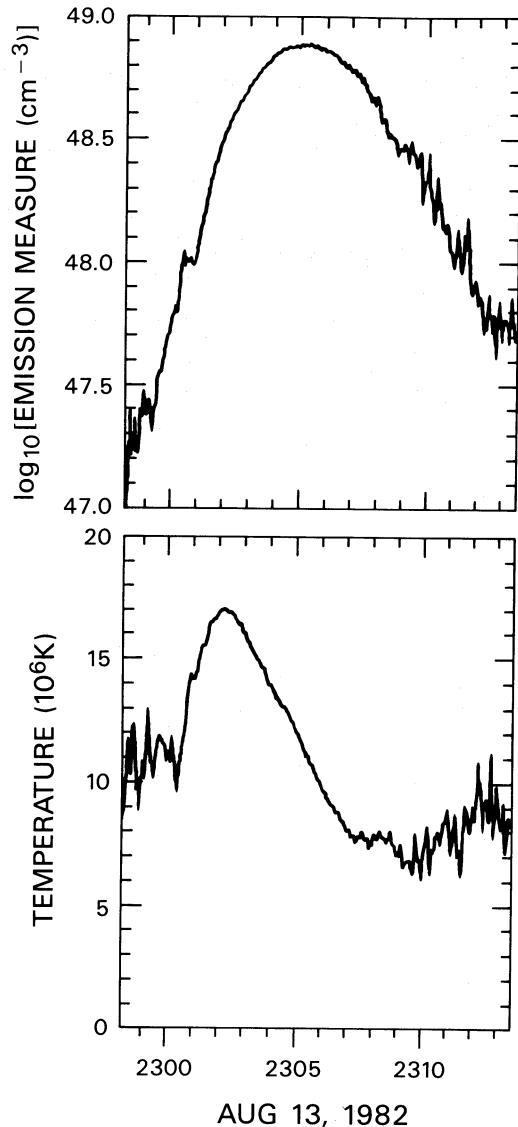


FIG. 6.—Variation of the temperature and emission measure during the 1982 August 13 event using *GOES* soft X-ray data. Compare Fig. 3.

Figure 6 shows the time variation of temperature and emission measure as derived from the *GOES* data during the same 1982 August 13 event that was shown in Figures 3 and 5.

If we assume, *a priori*, that the hard X-ray time profile describes the profile of particle acceleration in these events, then the delay to the peak of the 2 MHz radio data would represent the time required for electrons to propagate out to $\sim 6 R_{\odot}$, and the delay to the soft X-ray peak would represent the time required for the accelerated particles to heat the low corona. This simplistic picture leads us to choose the time of hard X-ray maximum of the dominant 2 MHz radio peak to determine the soft X-ray properties that might be most representative of the ambient conditions seen by the particles being accelerated. Consequently, the *ISEE* temperature and emission measure listed in Table 1 and used in later correlation plots were calculated at the time of the hard X-ray maximum corresponding to the largest radio event. These parameters were determined from the *ISEE* data since the sensitivity of the *GOES* detector was generally too low to allow the accurate

determination of the parameters at these early times in the flares.

For those events without hard X-rays, we used the average hard X-ray to 2 MHz radio peak delay of approximately 1 minute to determine the time at which the temperature and emission measure were calculated. For the 1979 May 17 event shown in Figure 4, the single small X-ray peak was used since that was the only possible time and the event is of particular interest.

Table 1 shows the onset time of each event, the $^3\text{He}/^4\text{He}$ ratio and intensity, the *GOES* peak flux, the *ISEE* 5 Kev X-ray peak flux, emission measure, temperature and 25 keV peak rate, the HXRBS peak count rate, total count, and power-law spectral index, the metric type III intensity, the kilometer type III intensity expressed as the logarithm of the antenna temperature T_A at 2 MHz, and the location and importance of the H α flare.

III. RESULTS AND DISCUSSION

The degree of correlation of the $^3\text{He}/^4\text{He}$ ratio with various X-ray and radio parameters listed in Table 1 may be seen in Figures 7–11. Figures 7–10 show the $^3\text{He}/^4\text{He}$ ratio versus the 2 MHz intensity ($\log T_A$), the soft X-ray peak flux, soft X-ray emission measure, and the total count of hard X-rays, respectively. These four figures show a persistent tendency of decreasing $^3\text{He}/^4\text{He}$ ratio with increasing value of any of these four measures of the intensity of the event.

In contrast, Figure 11 shows no apparent correlation between the $^3\text{He}/^4\text{He}$ ratio and the soft X-ray temperature.

Table 2 shows correlation coefficients corresponding to the data plotted in the figures and shown in Table 1. The number of events contributing to each coefficient is shown in Table 2 as is the correlation probability when that probability is greater than 90%. Correlation with the ^3He intensity might also be of interest except that the ^3He intensity is strongly affected by the degree of magnetic connection between the event and Earth.

The data in Table 2 quantify the persistent negative correlation of the $^3\text{He}/^4\text{He}$ ratio with nearly all measures of the intensity of the parent event. Evidently the mechanism leading to ^3He enhancement operates preferentially in small events.

Fluctuations in the hard X-ray flux, like those shown in Figure 5, and the multiplicity of peaks seen in other X-ray and radio data reveal an underlying complexity in these events that cannot be characterized in the few broad parameters that we have been able to examine here. It is, therefore, no surprise that there is substantial nonstatistical scatter in the plots in Figures 7–10. It is, in fact, surprising that any correlation survives the process of averaging over the event or selecting a single peak among several. Perversely, the anticorrelation suggests that our choice of peak times to measure parameters is not correct, i.e., small events in a multievent sequence could contribute more ^3He than large ones. Fortunately, the variations with event size dependence is not precipitous and the correlation does not depend strongly on the choice of time at which the event parameters are measured.

The existence of a correlation between the $^3\text{He}/^4\text{He}$ ratio and the intensity of the event would not be expected for an acceleration mechanism with temporally decoupled preheating and acceleration phases such as the mechanism suggested by Fisk (1978; see also Varvoglis and Papadopoulos 1983). This conclusion was also reached by Kocharov and Dvoryanchikov (1985) based upon the observed correlation between $^3\text{He}/^4\text{He}$ and the ^3He spectral index. If the ^3He

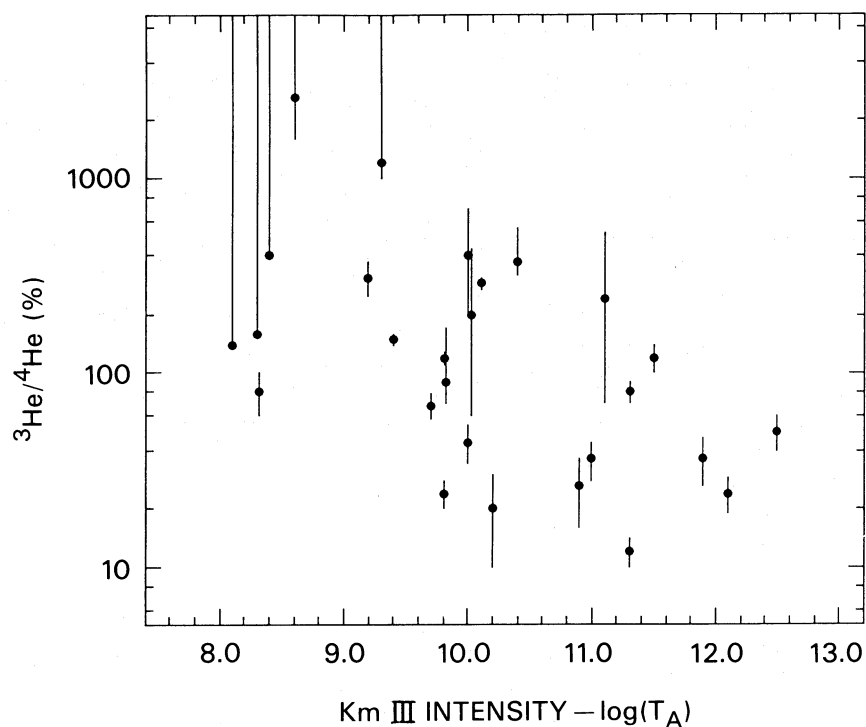


FIG. 7.—Plot of the $^3\text{He}/^4\text{He}$ ratio versus the kilometric radio intensity (log of antenna temperature) at 2 MHz

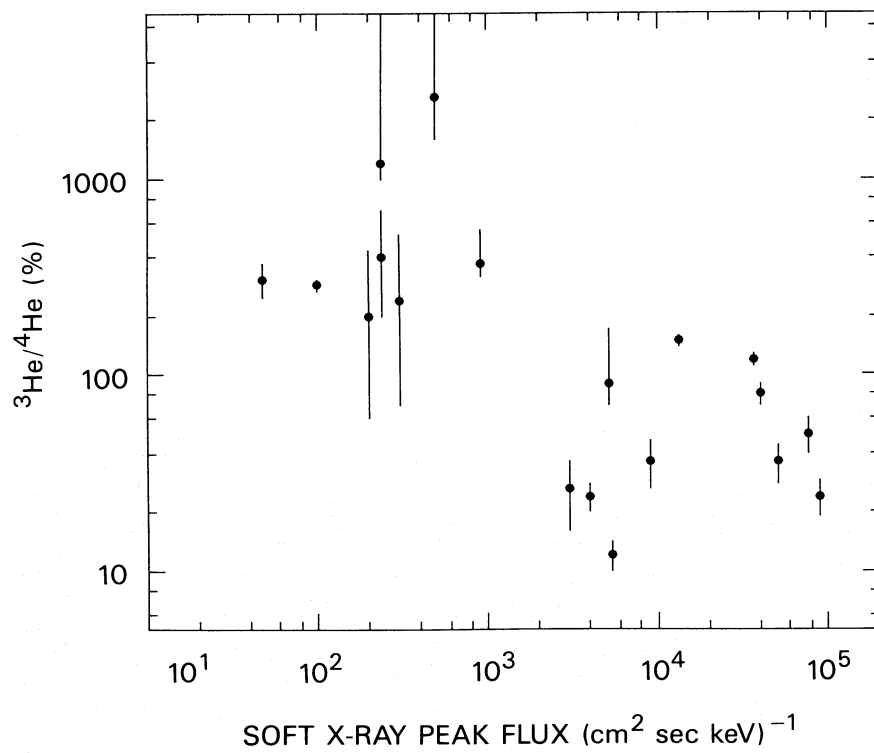


FIG. 8.—Plot of the $^3\text{He}/^4\text{He}$ ratio versus the ISEE 3 5 keV X-ray peak flux

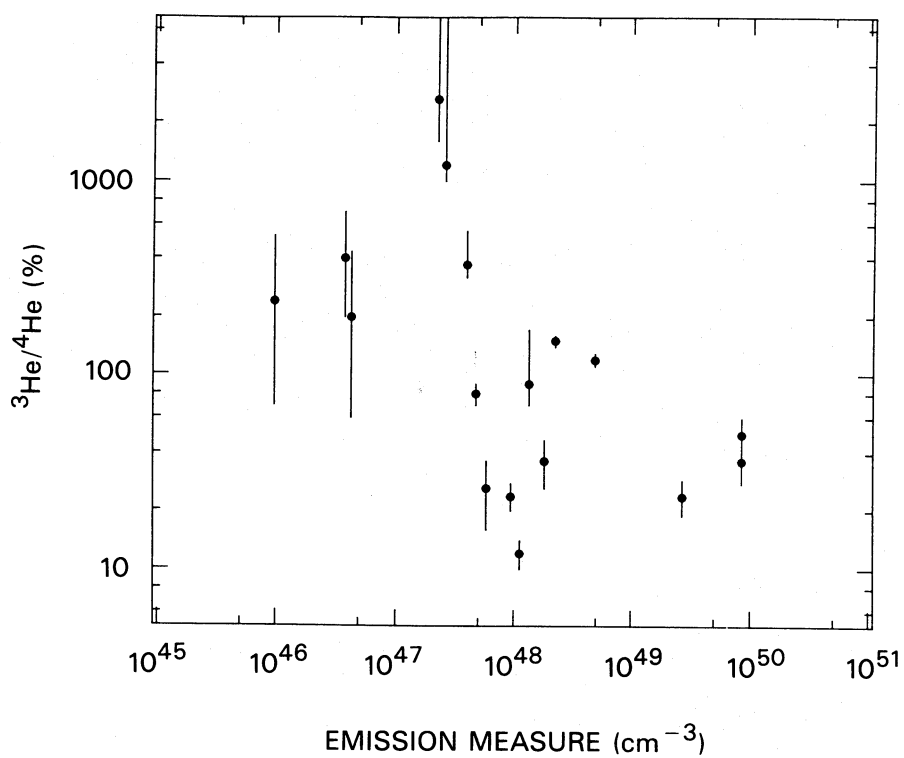


FIG. 9.—Plot of the $^3\text{He}/^4\text{He}$ ratio versus the *ISEE 3* soft X-ray emission measure at the time of the dominant hard X-ray maximum (see text)

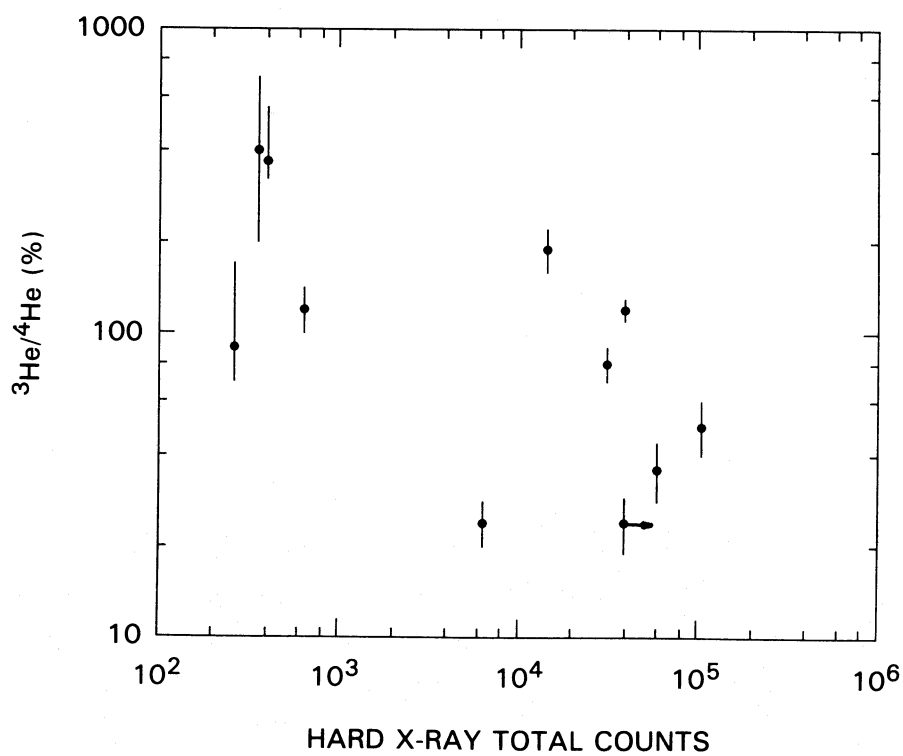


FIG. 10.—Plot of the $^3\text{He}/^4\text{He}$ ratio versus the HXRBS hard X-ray integral photon count

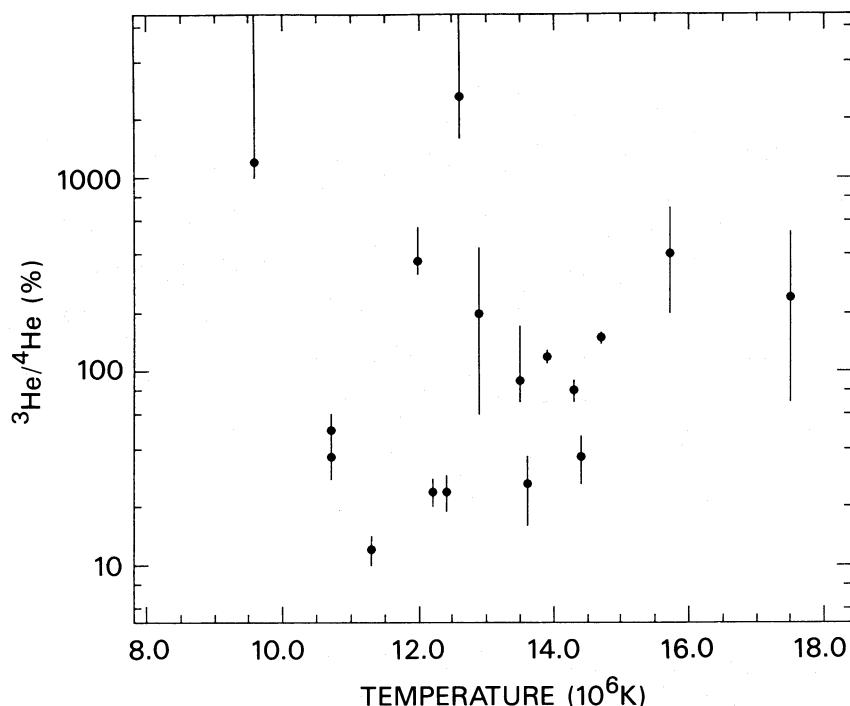


FIG. 11.—Plot of the $^3\text{He}/^4\text{He}$ ratio versus *ISEE 3* soft X-ray temperature at the time of the dominant hard X-ray maximum (see text). Unlike Figs. 7–10, there is no evidence of correlation in this figure.

enhancement occurs by preferential absorption of waves, then those waves could operate *during* the acceleration event when the intensities and spectra are being determined. It is also possible that the Fisk (1978) mechanism is simply more efficient in small flares where more moderate currents and a favorable electron-temperature to ion-temperature ratio might be expected.

The ^3He -rich events have been associated with small compact flares (Kahler *et al.* 1987), and they have been contrasted with the large long-duration flares that produce proton events (Reames and Stone 1986) which have particle abundances more nearly representative of the solar corona. It is possible that the waves that heat ^3He are produced in a compact region; a disturbance propagating outward from that region in intense flares could accelerate a component with ambient abundances that mixes with the enhanced component to dilute the $^3\text{He}/^4\text{He}$ ratio.

This mixing hypothesis would seem to suggest that increas-

ingly strong coronal shocks might be observed in increasingly intense events. Only the last event in Table 1 had a sufficiently intense shock to emit a metric type II radio burst; this event does have one of the lowest $^3\text{He}/^4\text{He}$ ratios in the table, however.

At present our explanation of the observed correlations is tentative and our understanding of the ^3He enhancements is incomplete. The lack of a clear *positive* correlation between the $^3\text{He}/^4\text{He}$ ratio and a property of the parent flare emphasizes the fact that we have yet to isolate any observable consequence of physical mechanism that leads to such extreme isotopic enhancements.

The authors are indebted to S. R. Kane for providing unpublished *ISEE* X-ray data and to H. Garcia for his assistance with the *GOES* X-ray data. A portion of this work was performed under NASA grants NAG5-376 and NGL-05-003-017.

TABLE 2
CORRELATION WITH $\log(^3\text{He}/^4\text{He})$

		Coefficient	Events (number)	Probability (%)
Soft X-rays:				
Temperature	[ISEE]	0.091	17	...
log (emission measure)	[ISEE]	-0.534	17	97
log (peak flux)	[ISEE]	-0.664	19	99
log (peak flux)	[GOES]	-0.550	16	97
Hard X-rays:				
log (peak rate)	[ISEE]	-0.494	14	93
log (peak rate)	[SMM]	-0.609	10	94
log (total counts)	[SMM]	-0.576	10	93
Spectral index	[SMM]	0.144	7	...
Radio:				
km type III log (T_A)	[ISEE]	-0.520	27	99

REFERENCES

- Anderson, K. A., Kane, S. R., Primbsch, J. H., Weitzmann, R. H., Evans, W. D., Klebesadel, R. W., and Aiello, W. P. 1978, *IEEE Trans.*, **GE-16**, 157.
- Dennis, B. R. 1985, *Solar Phys.*, **100**, 465.
- Dennis, B. R., Orwig, L. E., Kiplinger, A. L., Gibson, B. R., Kennard, G. S., and Tolbert, A. K. 1985, NASA TM-86236 (unpublished).
- Fisk, L. A. 1986, *Ap. J.*, **224**, 1048.
- Kahler, S. W., Lin, R. P., Reames, D. V., Stone, R. G., and Liggett, M. 1987, *Solar Phys.*, **107**, 385.
- Kocharov, L. G., and Dvoryanchikov, Ya. V. 1985, in *Proc. 19th Internat. Cosmic Ray Conf.* (La Jolla), (NASA CP-2376), **4**, 209.
- Kocharov, L. G., and Kocharov, G. E. 1984, *Space Sci. Rev.*, **38**, 89.
- Orwig, L. E., Frost, K. J., and Dennis, B. R. 1980, *Solar Phys.*, **65**, 25.
- Ramaty, R., et al. 1980, in *Solar Flares, A Monograph from the Skylab Solar Workshop II*, ed. P. A. Sturrock (Boulder: Colorado Associated University Press), p. 117.
- Reames, D. V., and Stone, R. G. 1986, *Ap. J.*, **308**, 902.
- Reames, D. V., von Rosenvinge, T. T., and Lin, R. P. 1985, *Ap. J.*, **292**, 716 (RvL).
- Thomas, R. J., Starr, R., and Crannell, C. J. 1985, *Solar Phys.*, **95**, 323.
- Varvoglis, H., and Papadopoulos, K. 1983, *Ap. J. (Letters)*, **270**, L95.

B. R. DENNIS: Code 682, NASA/Goddard Space Flight Center, Greenbelt, MD 20771

R. P. LIN: Space Sciences Laboratory, University of California, Berkeley, CA 94720

D. V. REAMES: Code 661, NASA/Goddard Space Flight Center, Greenbelt, MD 20771

R. G. STONE: Code 690, NASA/Goddard Space Flight Center, Greenbelt, MD 20771